JOC Article
pubs.acs.org/joc

Total Synthesis of Natural and Non-Natural $\Delta^{5,6}\Delta^{12,13}$-Jatrophane Diterpenes and Their Evaluation as MDR Modulators

Christoph Schnabel,[†] Katja Sterz,[‡] Henrik Müller,[‡] Julia Rehbein,[†,§] Michael Wiese,*[,‡] and Martin Hiersemann*[,†]

[†]*Technische Universität Dortmund, Fakultät Chemie, D-44227 Dortmund, Germany, and* [‡]*Universität Bonn, Pharmazeutisches Institut, Pharmazeutische Chemie II, D-53121 Bonn, Germany.* [§]*Present address: Physical Organic Chemistry Centre, School of Chemistry, Cardiff University, Cardiff CF10 3AT, U.K.*

m.wiese@uni-bonn.de; martin.hiersemann@udo.edu

Received October 12, 2010

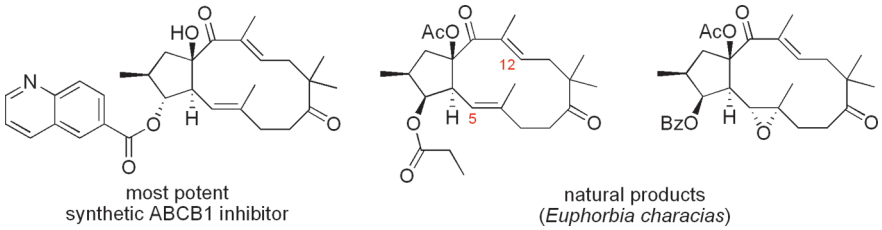

We report the details of the total synthesis of natural and non-natural jatropha-5,12-dienes. The successful tactic for the assembly of the strained *trans*-bicyclo[10.3.0]pentadecane scaffold employed a *B*-alkyl Suzuki−Miyaura cross-coupling for the formation of the C5/C6 double bond and a ring-closing metathesis for the construction of the C12/C13 double bond. The key step of the synthesis of the cyclopentane fragment, an uncatalyzed intramolecular carbonyl−ene reaction, was studied computationally by DFT calculations. The members of the ensemble of synthetic natural and non-natural jatrophanes were subsequently examined as modulators for the ABCB1, ABCG2, and ABCC1 efflux proteins, which are associated with multidrug resistance in cancer chemotherapy.

Introduction

According to a recent review, more than 150 different jatrophane diterpenes have thus far been isolated from plants of the genus *Euphorbia*.[1] Based on a unique *trans*-bicyclo[10.3.0]-pentadecane skeleton, the fascinating structural diversity of jatrophanes originates from the degree of hydroxylation and acyloxylation as well as configurational permutation. Given the well-documented phytopharmacological importance of the genus *Euphorbia* since ancient times, it comes to no surprise that a broad range of biological properties have been reported for constituents of the plant extract.[2] In particular, jatrophane diterpenes have been characterized as "potent and specific P-glycoprotein modulators".[3] The interesting biological properties and the unusual molecular architecture of jatrophane diterpenes from *Euphorbia* sp. have attracted considerable interest, leading to several synthetic studies and one completed total synthesis.[4,5]

Within the family of jatrophane diterpenes, a structural branch is distinguished by the *trans*-bicyclo[10.3.0]pentadecane scaffold and double bonds between C5/C6 and C12/C13 (Figure 1); the members of this subfamily, jatropha-5,12-dienes **1a**−**k**, have been isolated from *E. characias*,[6] *E. pubescens*,[7] and *E. helioscopia*.[3,8] In addition to their fascinating structure, **1d**−**f**,**i** possess P-glycoprotein modulating

(1) Shi, Q. W.; Su, X. H.; Kiyota, H. *Chem. Rev.* **2008**, *108*, 4295–4327.
(2) Hiller, K.; Melzig, M. F. *Lexikon der Arzneipflanzen und Drogen*; Spektrum Akademischer Verlag: Heidelberg, Germany, 1999.
(3) Barile, E.; Borriello, M.; Pietro, A. D.; Doreau, A.; Fattorusso, C.; Fattorusso, E.; Lanzotti, V. *Org. Biomol. Chem.* **2008**, *6*, 1756–1762.
(4) For synthetic studies, see: (a) Helmboldt, H.; Rehbein, J.; Hiersemann, M. *Tetrahedron Lett.* **2004**, *45*, 289–292. (b) Gilbert, M. W.; Galkina, A.; Mulzer, J. *Synlett* **2004**, 2558–2562. (c) Mulzer, J.; Giester, G.; Gilbert, M. *Helv. Chim. Acta* **2005**, *88*, 1560–1579. (d) Helmboldt, H.; Köhler, D.; Hiersemann, M. *Org. Lett.* **2006**, *8*, 1573–1576. (e) Shimokawa, K.; Takamura, H.; Uemura, D. *Tetrahedron Lett.* **2007**, *48*, 5623–5625. (f) Helmboldt, H.; Hiersemann, M. *J. Org. Chem.* **2009**, *74*, 1698–1708. (g) Lentsch, C.; Rinner, U. *Org. Lett.* **2009**, *11*, 5326–5328.
(5) For the first total synthesis of a jatrophane diterpene from *Euphorbia* sp., see: Schnabel, C.; Hiersemann, M. *Org. Lett.* **2009**, *11*, 2555–2558.
(6) Seip, E. H.; Hecker, E. *Phytochemistry* **1984**, *23*, 1689–1694.
(7) (a) Valente, C.; Ferreira, M. J. U.; Abreu, P. M.; Pedro, M.; Cerqueira, F.; Nascimento, M. S. J. *Planta Med.* **2003**, *69*, 361–366. (b) Valente, C.; Ferreira, M. J. U.; Abreu, P. M.; Gyemant, N.; Ugocsai, K.; Hohmann, J.; Molnar, J. *Planta Med.* **2004**, *70*, 81–84.
(8) (a) Yamamura, S.; Shizuri, Y.; Kosemura, S.; Ohtsuka, J.; Tayama, T.; Ohba, S.; Ito, M.; Saito, Y.; Terada, Y. *Phytochemistry* **1989**, *28*, 3421–3436. (b) Zhang, W.; Guo, Y.-W. *Planta Med.* **2005**, *71*, 283–286. (c) Zhang, W.; Guo, Y.-W. *Chem. Pharm. Bull.* **2006**, *54*, 1037–1039.

Published on Web 12/30/2010 DOI: 10.1021/jo1019738

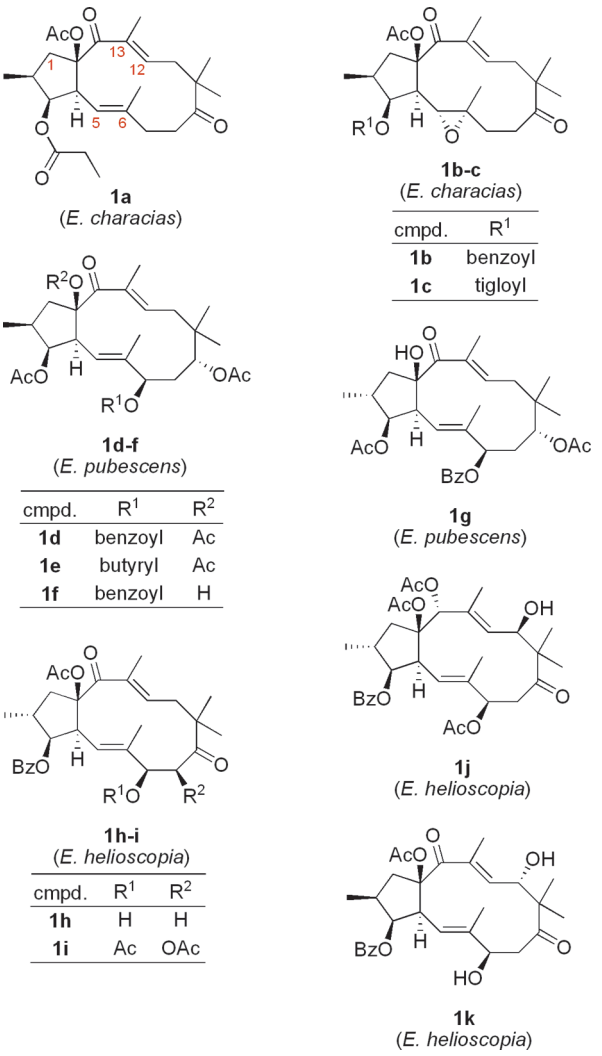

FIGURE 1. $\Delta^{5,6}\Delta^{12,13}$-Jatrophanes from plants of the genus *Euphorbia*.

properties and **1d**−**f** exhibit a moderate growth-inhibitory effect on the NCI-H460 human lung cancer cell line.[7a,b]

In this article we outline details of our initial report on the total synthesis of the jatropha-5,12-diene **1a**,[5] including failed tactics, unexpected reactivities, and a computational analysis of the stereochemical course of the intramolecular carbonyl−ene reaction utilized for the construction of the cyclopentane moiety. Furthermore, we outline the first total synthesis of **1b** as well as the syntheses of a collection of non-natural jatropha-5,12-dienes. Finally, we report the results of a biological evaluation of the inhibitory activity of synthesized jatrophanes toward ABCB1 (P-gp), ABCC1 (MRP1), and ABCG2 (BCRP), the three major transport proteins involved in the multidrug resistance (MDR) of tumor cells.

Results and Discussion

With the intention to develop a successful synthetic strategy to the carbon backbone of jatropha-5,12-dienes, we selected the diester **1a** and the related epoxide **1b** as initial targets. Taking advantage of experiences from previous synthetic approaches,[4] we devised a synthetic strategy that is outlined in Scheme 1. A posteriori, it turned out that the diol **2**,

SCHEME 1. Retrosynthesis of 1a,b

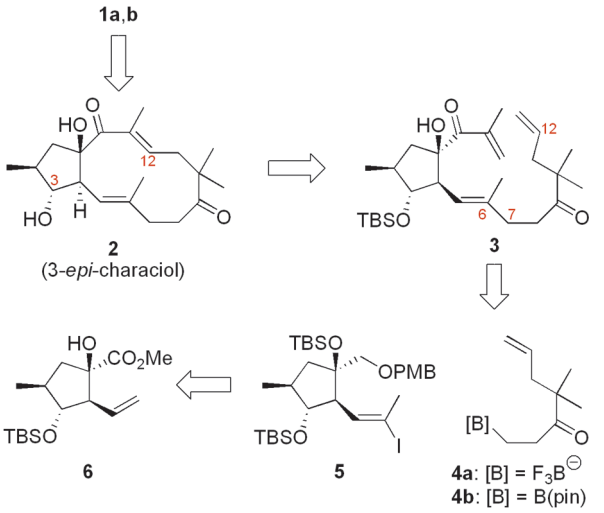

named 3-*epi*-characiol (**2**) according to Seip and Hecker,[6] represents a versatile late-stage intermediate for the synthesis of the natural jatrophanes **1a**,**b** as well as a collection of non-natural derivatives. Because the stereochemical complexity of 3-*epi*-characiol (**2**) is located at the 5-membered ring, we were lured to the initial development of a scalable access to a suitable cyclopentane building block; consequently, this course of action would require a tactic for the annulation of the 12-membered ring onto the existing 5-membered ring. It is important to consider that the ring-closing operation has to outmaneuver the energetic consequences of the conformational rigidity of the 12-membered ring which is caused by the trans connectivity and the presence of two trisubstituted *E*-configured double bonds, one of which is part of an enone. After having experienced the failure of ring-closing operations between C5/C6 (ring-closing metathesis, RCM), C8/C9 (dithiane alkylation), and C13/C14 (Ad_{Nu}),[4] we opted for the application of a ring-closing transform to disconnect the C12/C13 double bond. The subsequent structural simplification of the resulting triene **3** was guided by a convergent tactic: namely, the merger of the vinyl iodide **5** and the organotrifluoroborate **4a** or the boronic acid ester **4b** by a cross-coupling reaction. Our retrosynthetic endgame then envisioned the disassembly of the vinyl iodide **5** to the terminal olefin **6**, for which a synthetic access was already established.

Intramolecular Carbonyl−Ene Reaction. As previously reported, the synthesis of cyclopentane building block **6** requires nine steps and delivers the diastereomers **6** and **7** on a multigram scale (Scheme 2).[5] Key to the sequence is the uncatalyzed intramolecular carbonyl−ene reaction, which was performed by heating the α-keto ester **8** in decane in a sealed tube to 180 °C bath temperature for approximately 3 days (TLC control of product formation) and delivered, after removal of the solvent and chromatographic purification, the separated diastereomeric cyclopentanoids **6** (62%) and **7** (12%).[9] In an effort to improve our understanding of the factors determining diastereoselectivity in this transformation, we initiated further experimental and theoretical

(9) This approach was inspired by chemistry previously reported from our laboratory; see: Hiersemann, M. *Eur. J. Org. Chem.* **2001**, 483–491.

SCHEME 2. Intramolecular Carbonyl−Ene Reaction

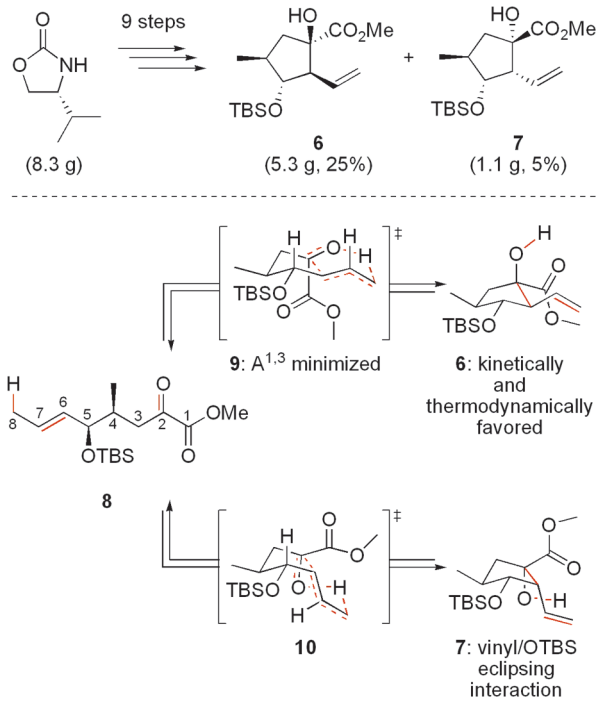

studies. With regard to thermodynamics, we found that the ene reaction is reversible and that **6** is the predominant component of the equilibrium mixture, which consists of **6**, **7**, and a residual amount of **8** (**6**/**7** = 85/15, $\Delta\Delta G^{r}$ = 1.6 kcal at 180 °C); experimentally, we routinely recycled the minor diastereomer **7** by subjecting it to the original conditions of the ene reaction, a procedure that provides a synthetically useful mixture of chromatographically separable diastereomers (**6**/**7** = 85/15). With respect to kinetics, the determination of the initial first-order rate constants for the ene reaction indicated that the formation of **6** over **7** is favored not only thermodynamically but kinetically as well ($\Delta\Delta G^{\ddagger}$ = 1.7 kcal/mol at 180 °C). We then hypothesized that the uncatalyzed ene reaction proceeds by a concerted bond reorganization process via the competing transition-state structures **9** and **10** to afford the diastereomeric cyclopentanoids **6** and **7** (Scheme 2).

Using the Gaussian03 suite of programs,[10,11] we employed the meta hybrid GGA functional B1B95[12] in combination

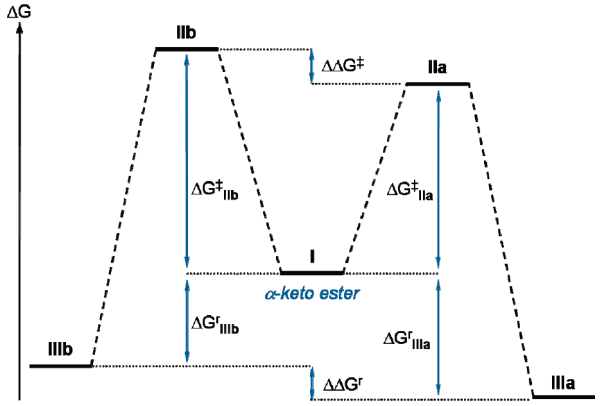

FIGURE 2. Free energy profile computed by DFT calculations. Free energy values are given in Table 1.

with the double-ζ basis set 6-31G(d)[13] to locate the relevant structures depicted in the lower part of Scheme 2.[14,15] In order to limit the number of diastereomeric conformations, the *t*-BuMe$_2$Si protecting group was replaced with a Me$_3$Si group for the calculations. Thus, **I**, **IIa**/**b**, and **IIIa**/**b** represent simplified models for **8**, **9**/**10**, and **6**/**7** (Figure 2). The fully optimized structures of **I**−**III** were subjected to harmonic frequency analysis, and the resulting free energies (ΔG in kcal/mol) were used for comparison with the estimated experimental values (vide supra). According to the results of the gas-phase calculations at 298.15 K (Table 1, entry 1), a thermodynamic ($\Delta\Delta G^{r}$ = 2.5 kcal/mol) and kinetic ($\Delta\Delta G^{\ddagger}$ = 0.5 kcal/mol) preference for the formation of **IIIa** versus **IIIb** from **I** is predicted in reasonable accordance with the approximated experimental values at 180 °C in decane (vide supra). Furthermore, the B1B95/6-31G(d) calculated ΔG^{r} values for **IIIa** (−1.7 kcal/mol) and **IIIb** (+0.8 kcal/mol) are in good agreement with the experimental values. In order to account for implicit solvation effects and the reaction temperature effect on ΔG^{r}, calculations at the B1B95/6-31G(d)+PCM level at 453 K were performed and afforded a $\Delta\Delta G^{r}$ value (1.6 kcal/mol) which corresponds to the experimental value (Table 1, entry 2). We note that B1B95/6-31G(d) gas-phase single-point calculations at 453 K provided the least accurate values for $\Delta\Delta G^{\ddagger}$ (0 kcal/mol) and $\Delta\Delta G^{r}$ (2.8 kcal/mol) (Table 1, entry 3). We subsequently studied the influence of the basis set size on the calculated thermochemistry of the intramolecular carbonyl−ene reaction. Toward this end, structure optimizations and harmonic frequency calculations were performed using the B1B95 functional in connection with the 6-31+G(d,p) and 6-311++G(d,p) basis sets (Table 1, entries 4 and 5). In comparison with the B1B95/6-31G(d) calculation, the addition of p functions to hydrogen atoms and diffuse

(10) Gaussian03/E.01: Frisch, M. J.; Trucks, G. W.; Schlegel, H. B.; Scuseria, G. E.; Robb, M. A.; Cheeseman, J. R.; Montgomery, J. A., Jr.; Vreven, T.; Kudin, K. N.; Burant, J. C.; Millam, J. M.; Iyengar, S. S.; Tomasi, J.; Barone, V.; Mennucci, B.; Cossi, M.; Scalmani, G.; Rega, N.; Petersson, G. A.; Nakatsuji, H.; Hada, M.; Ehara, M.; Toyota, K.; Fukuda, R.; Hasegawa, J.; Ishida, M.; Nakajima, T.; Honda, Y.; Kitao, O.; Nakai, H.; Klene, M.; Li, X.; Knox, J. E.; Hratchian, H. P.; Cross, J. B.; Bakken, V.; Adamo, C.; Jaramillo, J.; Gomperts, R.; Stratmann, R. E.; Yazyev, O.; Austin, A. J.; Cammi, R.; Pomelli, C.; Ochterski, J. W.; Ayala, P. Y.; Morokuma, K.; Voth, G. A.; Salvador, P.; Dannenberg, J. J.; Zakrzewski, V. G.; Dapprich, S.; Daniels, A. D.; Strain, M. C.; Farkas, O.; Malick, D. K.; Rabuck, A. D.; Raghavachari, K.; Foresman, J. B.; Ortiz, J. V.; Cui, Q.; Baboul, A. G.; Clifford, S.; Cioslowski, J.; Stefanov, B. B.; Liu, G.; Liashenko, A.; Piskorz, P.; Komaromi, I.; Martin, R. L.; Fox, D. J.; Keith, T.; Al-Laham, M. A.; Peng, C. Y.; Nanayakkara, A.; Challacombe, M.; Gill, P. M. W.; Johnson, B.; Chen, W.; Wong, M. W.; Gonzalez, C.; Pople, J. A. *Gaussian03, Rev. C.02*; Gaussian, Inc., Wallingford, CT, **2004**.

(11) For computational details see the Supporting Information.

(12) Becke, A. D. *J. Chem. Phys.* **1996**, *104*, 1040–1046.

(13) (a) Hehre, W. J.; Ditchfield, R.; Pople, J. A. *J. Chem. Phys.* **1972**, *56*, 2257–2261. (b) Hariharan, P. C.; Pople, J. A. *Theor. Chim. Acta* **1973**, *28*, 213–222.

(14) For computational studies on the intramolecular carbonyl−ene reaction of unsaturated aldehydes and ketones, see: (a) Sauer, E. L. O.; Hooper, J.; Woo, T.; Barriault, L. *J. Am. Chem. Soc.* **2007**, *129*, 2112–2119. (b) Williams, J. T.; Bahia, P. S.; Kariuki, B. M.; Spencer, N.; Philp, D.; Snaith, J. S. *J. Org. Chem.* **2006**, *71*, 2460–2471. (c) Mondal, N.; Chakrabarty, K.; Roy, S.; Das, G. K. *J. Mol. Struct.* (*THEOCHEM*) **2004**, *684*, 187–195. (d) Chakrabarty, K.; Roy, S.; Das, G. K. *J. Mol. Struct.* (*THEOCHEM*) **2006**, *760*, 203–207. (e) Chakrabarty, K.; Roy, S.; Das, G. K.; Mondal, N. *J. Mol. Struct.* (*THEOCHEM*) **2007**, *805*, 1–7.

(15) B3LYP/6-31G(d) and M05−2X/6-31G(d) calculations provided unrealistic reaction free energies. See the Supporting Information for details.

TABLE 1. Calculated Thermochemistry of the Intramolecular Carbonyl−Ene Reaction

entry	method	$\Delta G^{\ddagger}_{\mathbf{IIa}}$	$\Delta G^{\ddagger}_{\mathbf{IIb}}$	$\Delta\Delta G^{\ddagger}$	$\Delta G^{r}_{\mathbf{IIIa}}$	$\Delta G^{r}_{\mathbf{IIIb}}$	$\Delta\Delta G^{r}$
1	B1B95/6-31G(d)	+33.1	+33.6	0.5	−1.7	+0.8	2.5
2	B1B95/6-31G(d)+PCM[a]				+1.2	+2.8	1.6
3	B1B95/6-31G(d)[b]	+35.7	+35.7	0	−0.7	+2.1	2.8
4	B1B95/6-31+G(d,p)	+31.6	+33.3	1.7	−4.6	−2.6	2.0
5	B1B95/6-311++G(d,p)	+29.7	+31.3	1.6	−6.4	−4.7	1.7

[a]Conditions: solvent heptane, temperature 453.15 K. [b]Conditions: temperature 453 K.

TABLE 2. Selected B1B95/6-31G(d) Interatomic Distances, C8−H−O Bond Angles (α), and O=C1−C2=O Dihedral Angles (ω)

entry	compd	d_{C8-H} (Å)	d_{C6-C2} (Å)	d_{O-H} (Å)	α (deg)[a]	ω (deg)[b]	$d_{OH\cdots O}$ (Å)
1	**I**	1.09				177	
2	**IIa**	1.32	2.03	1.29	156	134	
2′	**IIb**	1.30	2.01	1.32	155	156	
3	**IIIa**		1.55	0.97			1.98
3′	**IIIb**		1.56	0.97			2.00

[a]C8−H−O bond angle. [b]O=C1−C2=O dihedral angle.

TABLE 3. NBO Natural Atomic Charges of Selected Atoms of the α-Keto Ester Ia, the Diastereomeric Transition-State Structures IIa,b, and the Product Diastereomers IIIa,b Obtained from B1B95/6-31G(d) Calculations

entry	compd	O2	∼H∼	C2	C6	C7	C8
1	**I**	−0.50	+0.25	+0.51	−0.27	−0.21	−0.72
2	**IIa**	−0.66	+0.40	+0.34	−0.35	−0.12	−0.69
3	**IIb**	−0.66	+0.40	+0.33	−0.33	−0.10	−0.70
4	**IIIa**	−0.77	+0.50	+0.20	−0.33	−0.23	−0.43
5	**IIIb**	−0.77	+0.50	+0.20	−0.33	−0.22	−0.44

functions to heavy atoms decreases the reaction barrier via **IIa** (−1.5 kcal/mol lowering) and **IIb** (−0.3 kcal/mol lowering) and, hence, $\Delta\Delta G^{\ddagger}$ is increased to 1.7 kcal/mol (Table 1, entry 4). This value corresponds to the experimentally observed $\Delta\Delta G^{\ddagger}$ value at 180 °C in decane; furthermore, the computations at this level predict an increased exergonicity of the formation of **IIIa** ($\Delta G^{r} = -4.6$ kcal/mol) and **IIIb** ($\Delta G^{r} = -2.6$ kcal/mol). The resulting $\Delta\Delta G^{r}$ value in favor of **IIIa** (2.0 kcal/mol) is in good accordance with the experimental value (1.6 kcal/mol) at 180 °C in decane. Finally, we studied the impact of the 6-311++G(d,p) basis set on the B1B95 predicted thermochemistry (Table 1, entry 5). At this level, the lowest reaction barriers via **IIa** (29.7 kcal/mol) and **IIb** (31.3 kcal/mol) are prognosticated and the resulting $\Delta\Delta G^{\ddagger}$ value of 1.6 kcal/mol is close to the experimental value at 180 °C in decane (1.7 kcal/mol). Furthermore, a markedly exergonic carbonyl−ene process is predicted but the $\Delta\Delta G^{r}$ value in favor of **IIIa** (1.7 kcal/mol) corresponds to the experimental value (1.6 kcal/mol) at 180 °C in decane.

The experimentally observed kinetics and thermodynamics are most accurately modeled at the B1B95/6-31G(d) or B1B95/6-31+G(d,p) level. Next, we inspected selected geometric properties of the transition structures **IIa** and **IIb** with the intent to gain a glimpse into the origin of the kinetic diastereoselectivity in favor of **6** (Table 2, Figure 3). Interestingly, with the exception of the dihedral angle ω, the critical σ-bond lengths and the C8−H−O bond angle within the pericyclic array of reorganizing bonds are closely related for the competing transition-state structures **IIa** and **IIb** at all levels of theory (Table 2, entries 2 and 2′).[16] Additionally, the natural atomic charges on the atoms that are directly involved in the pericyclic event indicate a nearly identical charge distribution within the competing transition-state structures **IIa** and **IIb** (Table 3).[17] Therefore, we conclude that $\Delta\Delta G^{\ddagger}$ is not caused by differences in the nature of the concerted bond reorganization process. Which factors, then, contribute to the small but significant free energy difference between **IIa** and **IIb**? In our initial qualitative analysis, we had hypothesized that the difference in the extent of allylic strain could destabilize **9** relative to **10** (Scheme 2) and, in analogy, **IIa** to **IIb** (Figure 3). Use of the allylic strain concept for the qualitative evaluation of the relative stability of diastereomeric transition-state structures is not without precedent.[18,19] However, inspection of the calculated ground-state (**I**) and transition-state structures (**IIa**) revealed a significant geometric distortion of the allyl segment in **IIa**, which leads to a C7−C6−C5 bond angle of 120° and causes a conspicuous proximity of H7 and H5 (2.24 Å). This unfavorable arrangement is due to the geometric requirements of the strained bicyclic transition-state structure and casts doubt on the validity of our qualitative stereochemical model that relies exclusively on the conformational properties of the allyl element. Evidently more significant for the relative stability of **IIa** and **IIb** is the observation that the bicyclic transition-state structure **IIb** enforces a close proximity (2.15 Å) of the hydrogen atoms at C4 and C7. Hence, the results of the inspection of the geometric properties of the optimized structure of **IIa** and **IIb** support the hypothesis that 1,3-transannular interactions are mainly responsible for the experimentally observed and computationally predicted free energy difference in favor of **IIa**. The dominating transannular strain that destabilizes **IIb** relative to **IIa** is reflected by the short interatomic distance between H-4 and H-7.

As the utility of our ene reaction rests on the thermodynamic preference for the formation of **IIIa**, attempts were next due to relate the thermodynamic diastereoselectivity ($\Delta\Delta G^{r}$) to the structural differences between **IIIa** and **IIIb**. The calculated structures of **IIIa**,**b** resemble an envelope type of conformation; the α-hydroxy ester fragment is bridged by a hydrogen bond, the bulky TMSO group adopts a pseudoequatorial position, and the $A^{1,3}$ of the C6 vinyl substituent is minimized (Figure 3). The selected dihedral angles given in Table 4 are useful for an advanced conformational analysis of the calculated structures of the cyclopentanoids **IIIa**,**b**; notably, the reported dihedral angles are closely related at all levels of theory.[16] For the more stable diastereomer **IIIa**, C6 is the out-of-plane atom of the envelope-shaped cyclopentane conformer

(16) See the Supporting Information for B3LYP and M05-2X values. Calculated interatomic distances are virtually insensitive to the size of the basis set; see the Supporting Information for 6-31+G(d,p) and 6-311++G(d,p) values.

(17) Relative NBO atomic charges are virtually independent of the basis set size. See the Supporting Information for details.

(18) (a) Hoffmann, R. W. *Chem. Rev.* **1989**, *89*, 1841–1860. (b) Johnson, F. *Chem. Rev.* **1968**, *68*, 375–413.

(19) For a recent example, see: Zhou, Y.; Murphy, P. V. *Org. Lett.* **2008**, *10*, 3777–3780.

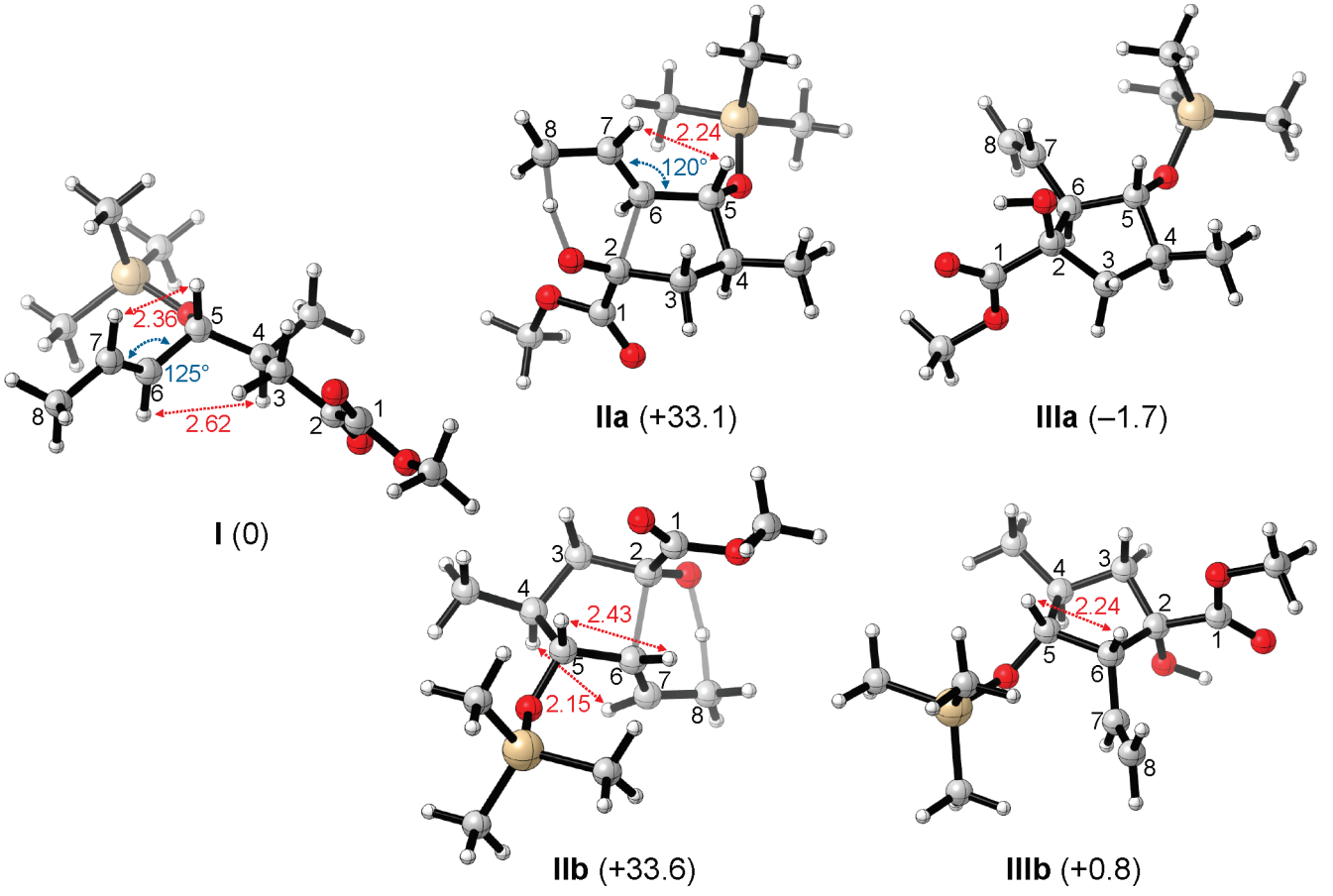

FIGURE 3. B1B95/6-31G* structural models. Interatomic distances are given in Å and bond angles in deg. Relative free energies in kcal/mol at 298.15 K.

TABLE 4. Selected B1B95/6-31G(d) Dihedral Angles (ω) of the Major (IIIa) and Minor (IIIb) Product Diastereomers

		ω (deg)	
entry	atoms	**IIIa**	**IIIb**
1	C2−C3−C4−C5	+9	+45
2	C4−C5−C6−C2	+46	0
3	O5′−C5−C4−C4′	+78	+83
4	C7−C6−C2−C1	+72	−85
5	O5′−C5−C6−C7	−71	−2

(Table 4, entry 1), whereas C3 is the out-of-plane atom for **IIIb** (Table 4, entry 2). A common structural property for **IIIa**,**b** is the synclinal orientation of the C4−Me and the C5−OTMS group (Table 4, entry 3). As a result of the different relative configurations of **IIIa**,**b**, the CO_2Me group and the vinyl substituent at C6 adopt different relative orientations (Table 4, entry 4); in **IIIb** the ester and the vinyl group are in an anticlinal orientation ($\omega_{C7-C6-C2-C1} = -85°$), whereas in **IIIa** the same substituents adopt a synclinal position ($\omega_{C7-C6-C2-C1} = +72°$). In terms of the strain-causing structural property that destabilizes **IIIb** relative to **IIIa**, it is conceivable that the eclipsed arrangement ($\omega_{O5'-C5-C6-C7} = -2°$) of the C4−OTMS and the C5−vinyl groups in **IIIb** is less favorable compared to the synclinal orientation ($\omega_{O5'-C5-C6-C7} = -71°$) of these two substituents in **IIIa** (Table 4, entry 5; Figure 3).

***B*-Alkyl Suzuki−Miyaura Cross-Coupling.** With the requisite cyclopentane building block **6** in hand, the next objective was to construct the substrates **4** and **5** for the projected cross-coupling reaction. Accordingly, we envisioned conversion of the aldehyde **11**, which was made available by resorting to a previously developed synthetic sequence from our group (Scheme 3),[5] into the vinyl iodide **5** by the hydrozirconation/iododezirconation of an internal alkyne.[20] Although we were intrigued by the prospect of a one-pot alkynylation/methylation sequence to access the required internal alkyne, our attempts to utilize the Corey−Fuchs protocol[21] (63%) or the Ohira−Bestmann reagent[22] (15%) for this purpose were disappointing. Therefore, we had to settle for a stepwise line of events in which the aldehyde **11** was subjected to a Wittig olefination to deliver a crude vinyl chloride which underwent elimination when treated with LDA to afford the terminal alkyne; application of *n*-BuLi instead of LDA was less satisfactory, causing extensive decomposition and inferior yield (50%). Following well-established chemistry for the construction of *E*-configured vinyl iodides, the terminal alkyne was subsequently treated with *n*-BuLi and the intermediate lithium acetylide was trapped with methyl iodide to provide the corresponding internal alkyne. Subsequent conversion of the internal alkyne into the vinyl iodide **5** was achieved in reasonable yield using an excess of the Schwartz

(20) Lipshutz, B. H.; Pfeiffer, S. S.; Noson, K.; Tomioka, T. In *Titanium and Zirconium in Organic Synthesis*; Marek, I., Ed.; Wiley-VCH: Weinheim, Germany, 2002; pp 110−148.
(21) Corey, E. J.; Fuchs, P. L. *Tetrahedron Lett.* **1972**, *13*, 3769–3772.
(22) (a) Ohira, S. *Synth. Commun.* **1989**, *19*, 561–564. (b) Müller, S.; Liepold, B.; Roth, G. J.; Bestmann, H. *Synlett* **1996**, 521–522.

SCHEME 3. Synthesis of the Vinyl Iodide 5

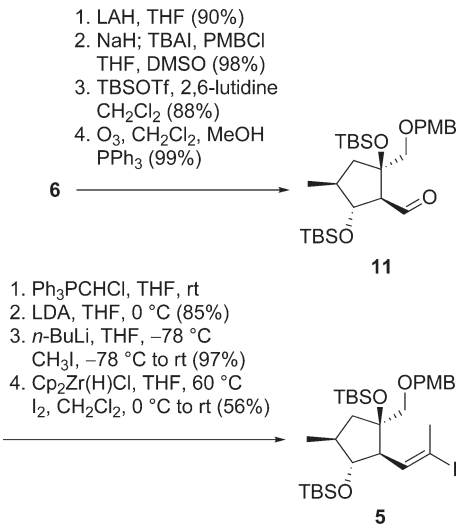

reagent[23] at elevated temperature to ensure the formation of a single regioisomer of the vinylzirconium intermediate.

Encouraged by the successful synthesis of the vinyl iodide **5**, we focused our efforts on the preparation of the projected cross-coupling partners, the organotrifluoroborate **4a** and boronate ester **4b** (Scheme 4). The commercial but expensive acid **13** was prepared from ethyl isobutyrate (**12**) by the allylation of the corresponding ester enolate followed by saponification of the crude ester to afford the acid **13**. The subsequent conversion of the acid **13** to the methyl ketone **14** proceeded uneventfully and set the stage for the introduction of the boronic acid ester moiety. For that purpose, pinacol iodomethaneboronate (**15**)[24,25] was prepared in analogy to a procedure by Brown[26] using MeLi[27] instead of *n*-BuLi for the iodine–lithium exchange reaction. With the electrophile **15** in hand, we subsequently investigated the alkylation of the methyl ketone **14**.[25] As we had hoped, exposure of ketone **14** to LDA and trapping of the intermediate enolate with **15** produced the *β*-boronate ketone **4b**, which was purified by chromatography on a gram scale. With the intent of harvesting the advertised advantages of organotrifluoroborates for Suzuki–Miyaura cross-coupling reactions,[28] the boronic acid ester **4b** was converted to the tetra-*n*-butylammonium organotrifluoroborate **4a** according to published procedures.[29,30]

With **4a**,**b** and **5** available, an investigation of the reaction conditions for their cross-coupling was conducted (Scheme 5). However, attempts to bring about the connection of the boronic acid ester **4b** and the vinyl iodide **5** in the presence of $(dppf)PdCl_2 \cdot CH_2Cl_2$, Ph_3As, and Cs_2CO_3 in DMF (or aqueous NaOH in THF) at elevated temperature were futile; notably, TLC control indicated the formation of a byproduct which was tentatively identified as the allene **16**. We

SCHEME 4. Synthesis of the Boronate 4a

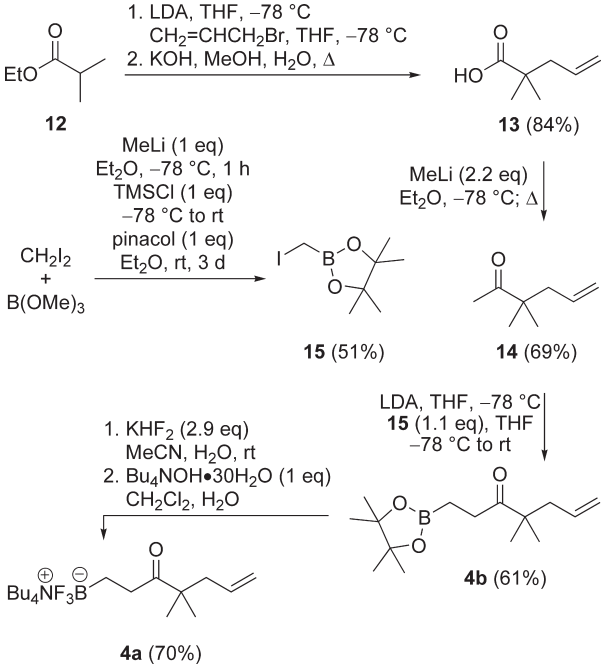

SCHEME 5. Unsuccessful Cross-Coupling Attempts

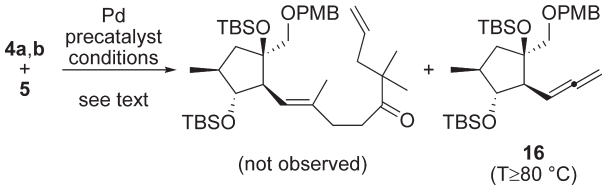

next turned our attention to the tetra-*n*-butylammonium organotrifluoroborate **4a** as a cross-coupling partner for the vinyl iodide **5**. However, when employing the reported conditions ($(dppf)PdCl_2 \cdot CH_2Cl_2$, Cs_2CO_3, toluene, H_2O, 80 °C),[31] the desired cross-coupling product was not observed, even if an excess of **4a** was used; instead, formation of the allene **16** was detected. Increasing the reaction temperature favored the formation of **16**; likewise, microwave irradiation was of no avail. Further unsuccessful modifications of the cross-coupling conditions involved different precatalysts ($Pd(OAc)_2$, $Pd(PPh_3)_4$), a change of solvent (*i*-PrOH), and the exclusion of water.[32]

Spurred by the unsuccessful cross-coupling between the *β*-boronate ketone **4a** and the vinyl iodide **5**, we decided to employ a triorganylborane for the projected *B*-alkyl Suzuki–Miyaura cross-coupling[33] and to resort to a less spacious protecting group for the diol moiety of the vinyl iodide. Accordingly, the acetonide **17** was synthesized from the initial carbonyl–ene reaction product **6** by a short sequence of high-yielding transformations (Scheme 6). Reduction of the α-hydroxy ester moiety and acetalization of the resulting 1,2-diol afforded an acetonide that was subjected to an ozonolysis of the terminal double bond to deliver an aldehyde

(23) Hart, D. W.; Schwartz, J. *J. Am. Chem. Soc.* **1974**, *96*, 8115–8116.
(24) (a) Wuts, P. G. M.; Thompson, P. A. *J. Organomet. Chem.* **1982**, *234*, 137–141. (b) Phillion, D. P.; Neubauer, R.; Andrew, S. S. *J. Org. Chem.* **1986**, *51*, 1610–1612.
(25) Mears, R. J.; Whiting, A. *Tetrahedron* **1993**, *49*, 177–186.
(26) Soundararajan, R.; Li, G.; Brown, H. C. *J. Org. Chem.* **1996**, *61*, 100–104.
(27) Wallace, R. H.; Zong, K. K. *Tetrahedron Lett.* **1992**, *33*, 6941–6944.
(28) Molander, G. A.; Ellis, N. *Acc. Chem. Res.* **2007**, *40*, 275–286.
(29) Vedejs, E.; Chapman, R. W.; Fields, S. C.; Lin, S.; Schrimpf, M. R. *J. Org. Chem.* **1995**, *60*, 3020–3027.
(30) Batey, R. A.; Quach, T. D. *Tetrahedron Lett.* **2001**, *42*, 9099–9103.
(31) Molander, G. A.; Ham, J.; Seapy, D. G. *Tetrahedron* **2007**, *63*, 768–775.
(32) Fürstner, A.; Larionov, O.; Flügge, S. *Angew. Chem.* **2007**, *119*, 5641–5644.
(33) Miyaura, N.; Ishiyama, T.; Ishikawa, M.; Suzuki, A. *Tetrahedron Lett.* **1986**, *27*, 6369–6372.

SCHEME 6. Synthesis of the Diol 19

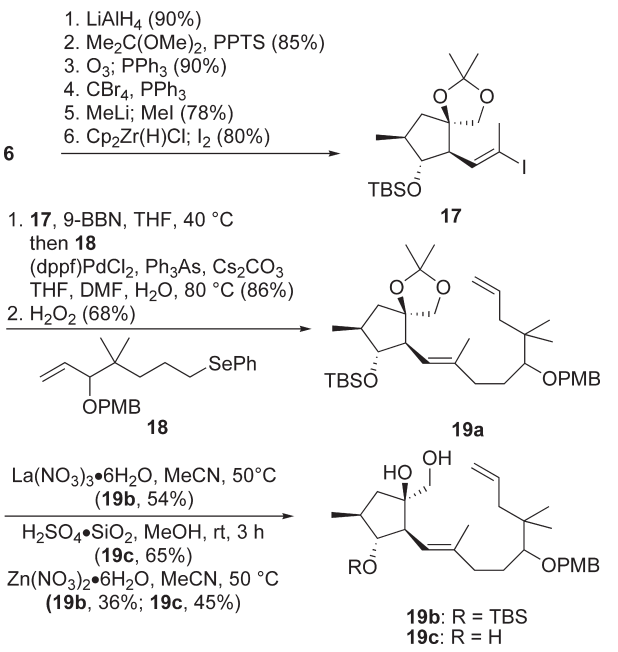

which was converted into a 1,1-dibromo olefin. Treatment of this 1,1-dibromo olefin with excess methyllithium (3.6 equiv) triggered a Fritsch−Buttenberg−Wiechell rearrangement to provide a lithium acetylide which was methylated in situ.[34] The resulting internal alkyne was then treated with the Schwartz reagent (3 equiv), and the intermediate vinylzirconium species was quenched with iodine to deliver the vinyl iodide **17** as a single regioisomer and diastereomer.

With the requisite substrates in hand, we proceeded to explore the key *B*-alkyl Suzuki−Miyaura cross-coupling reaction. The required triorganylborane was prepared in situ by the hydroboration of the olefin **18**, synthesized in five steps (45%) from 1,3-dibromopropane as previously reported,[5] with 9-borabicyclo[3.3.1]nonane[35] (9-BBN) at elevated temperature. Happily, without extensive need for optimization, applying the approved conditions[36] gave rise to the desired cross-coupling product in a usable and dependable yield. However, the utilization of **18** required us to unmask the terminal double bond needed for the RCM. Toward this end, the selenide from the successful cross-coupling reaction was oxidized to the selenoxide, which under the reaction conditions underwent a β-elimination to deliver the desired diene **19a** in moderate yield.[37] At this point, it was necessary to remove the acetal in order to introduce the missing isopropylidene moiety by nucleophilic addition to an α-hydroxy aldehyde. In this context, however, the presence of two other acid-labile hydroxyl protecting groups, TBS at C3 and PMB at C9, proved to be an underestimated challenge. Most obstructive was the sensitivity of the TBS protecting group under the Brønsted or Lewis acidic conditions required for the cleavage of an acetal. For instance, subjecting the acetal **19a** to

SCHEME 7. Synthesis of the Triene 21

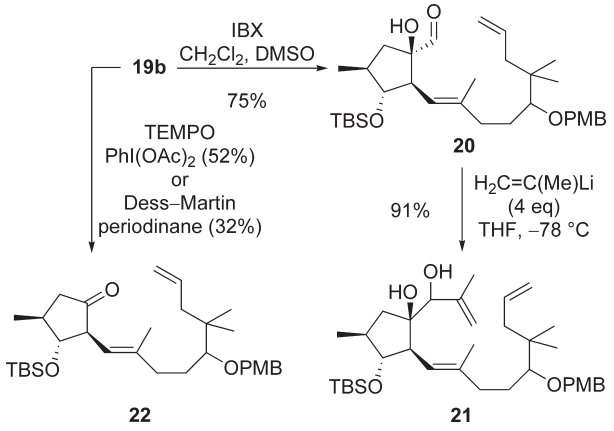

SCHEME 8. Benzilic Acid Like Rearrangement

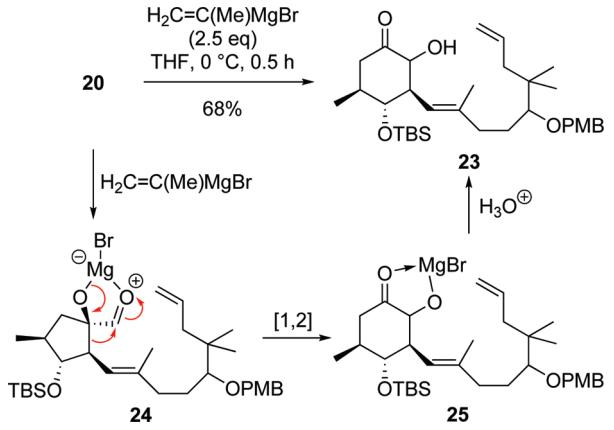

sulfuric acid on silica gel in methanol[38] led to the isolation of the triol **19c** and application of $Zn(NO_3)_2 \cdot 6H_2O$ in CH_3CN at elevated temperature[39] gave rise to a mixture of **19c** and the desired diol **19b**. Eventually, we found that subjecting **19a** to $La(NO_3)_3 \cdot 6H_2O$ in CH_3CN at elevated temperature was an acceptable procedure.[40] With the diol **19b** in hand, the next task became the oxidation to the corresponding α-hydroxy aldehyde **20** (Scheme 7). Initial attempts to utilize a TEMPO oxidation[41] or the Dess−Martin periodinane[42] led to oxidative cleavage of the diol and the formation of the ketone **22**. In accordance with literature reports, treatment of the diol **19a** with *o*-iodoxybenzoic acid (IBX) effected oxidation to the required α-hydroxy aldehyde **20**.[43] Subsequent nucleophilic addition of isopropenyllithium to the α-hydroxy aldehyde **20** delivered the allylic alcohol **21** as a mixture of diastereomers. Interestingly, the intended introduction of the isopropenyl group using commercial isopropenylmagnesium bromide unexpectedly afforded the α-hydroxy cyclohexanone **23**

(34) Knorr, R. *Chem. Rev.* **2004**, *104*, 3795–3850.
(35) Brown, H. C.; Knights, E. F.; Scouten, C. G. *J. Am. Chem. Soc.* **1974**, *96*, 7765–7770.
(36) Johnson, C. R.; Braun, M. P. *J. Am. Chem. Soc.* **1993**, *115*, 11014–11015.
(37) (a) Jones, D. N.; Mundy, D.; Whitehouse, R. D. *J. Chem. Soc.* **1970**, 86–87. (b) Sharpless, K. B.; Young, M. W. *J. Org. Chem.* **1975**, *40*, 947–949.
(38) Rajput, V. K.; Roy, B.; Mukhopadhyay, B. *Tetrahedron Lett.* **2006**, *47*, 6987–6991.
(39) Vijayasaradhi, S.; Singh, J.; Aidhen, I. S. *Synlett* **2000**, 110–112.
(40) Reddy, S. M.; Reddy, Y. V.; Venkateswarlu, Y. *Tetrahedron Lett.* **2005**, *46*, 7439–7441.
(41) De Mico, A.; Margarita, R.; Parlanti, L.; Vescovi, A.; Piancatelli, G. *J. Org. Chem.* **1997**, *62*, 6974–6977.
(42) (a) Dess, D. B.; Martin, J. C. *J. Org. Chem.* **1983**, *48*, 4155–4156. (b) Dess, D. B.; Martin, J. C. *J. Am. Chem. Soc.* **1991**, *113*, 7277–7287.
(43) (a) Frigerio, M.; Santagostino, M. *Tetrahedron Lett.* **1994**, *35*, 8019–8022. (b) Munari, S. D.; Frigerio, M.; Santagostino, M. *J. Org. Chem.* **1996**, *61*, 9272–9279.

SCHEME 9. Endgame toward 1a,b

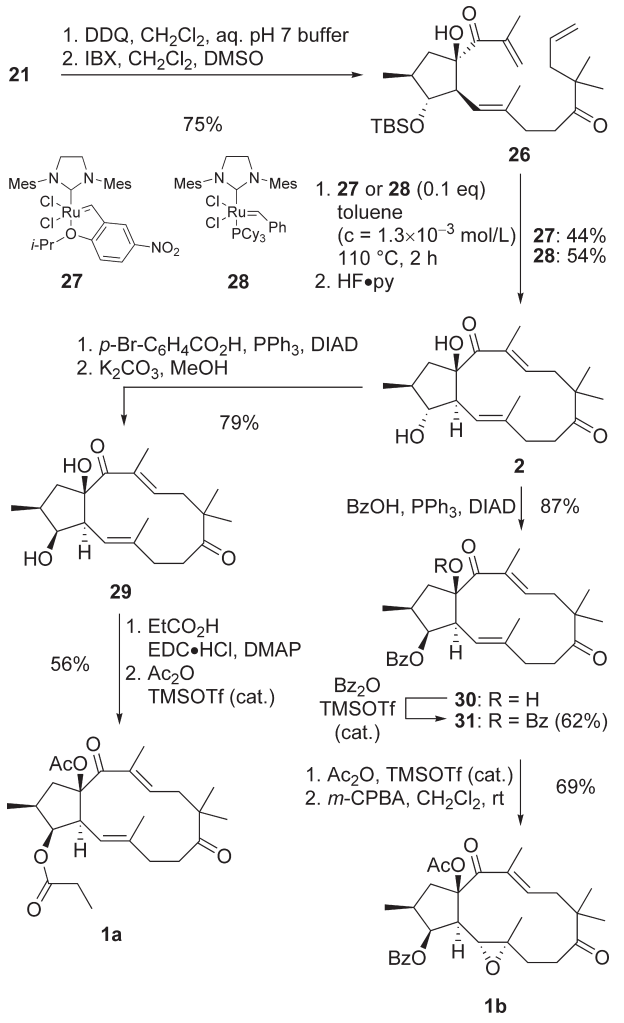

(Scheme 8). In order to explain the skeletal reorganization involved in the formation of **23**, we propose a nucleophilic [1,2] rearrangement of the intermediate chelate **24**, which corresponds to a variation of the benzilic acid rearrangement.[44]

With sufficient quantities of the triene **21** available, we were in a position to address the pivotal RCM. To this end, we decided to first remove the PMB protecting group and to oxidize the resulting triol to the diketone **26** (Scheme 9). Accordingly, a successful RCM of **26** would then establish the fully substituted *trans*-bicyclo[10.3.0]pentadecane framework of the jatropha-5,12-diene **1a**. Indeed, a sequence consisting of PMB protecting group removal under oxidative conditions[45] and IBX oxidation[43] was successful and delivered the diketone **26**. To our relief, the pivotal RCM could then be realized using the commercial precatalysts **27**[46] and **28**[47] at high temperature and afforded, after the removal of the remaining TBS protecting group with HF in pyridine, analytically pure 3-*epi*-characiol (**2**). In our hands, the Grela catalyst **27** performed slightly better than Grubbs' second-generation catalyst **28**. In additional experiments, we found that the Grubbs first-generation catalyst $Cl_2(Cy_3P)_2Ru{=}CHPh$[48] led to no conversion and that the Hoveyda−Grubbs catalyst[49] delivered inferior yields of **2** (22%).

Having happily reached for the first time an intermediate containing the complete carbon framework of jatropha-5,12-dienes, we decided to use 3-*epi*-characiol (**2**) as the starting point for structural diversification to natural and non-natural derivatives. Thus, conversion of **2** to characiol (**29**) was readily effected by Mitsunobu inversion[50] at C3 and subsequent transesterification (Scheme 9). The less sterically hindered, more reactive secondary hydroxyl group of **29** could be esterificated in 74% yield with propionic acid in the presence of *N*-ethyl-*N*′-(3-(dimethylamino)propyl)-carbodiimide hydrochloride (EDC·HCl) and DMAP.[51] Finally, the remaining tertiary hydroxyl group was successfully acetylated with Ac_2O in the presence of catalytic amounts of TMSOTf[52] to deliver the diester **1a** in 75% yield. Comparison of the ^{1}H NMR data of the resulting diester **1a** with the available data for the natural product revealed an excellent agreement. Considering the different frequencies at which the NMR spectra were recorded, the ^{1}H NMR spectrum (400 MHz) of synthetic **1a** was in good agreement with the available copy of the spectrum (90 MHz) of natural **1a**. The optical rotation of synthetic **1a** is −16.3° (*c* 0.4, $CHCl_3$); unfortunately, no literature value is available for **1a**. The assignment of the relative configuration by Seip and Hecker at that time relied exclusively on the comparison of the chemical shifts and coupling constants for H-1, H-2, and H-3 for **1a** and the lathyrane diterpene 5,6-epoxy-jolkinol. It now appears that our synthesis convincingly corroborates the original assignment of the constitution and relative configuration of natural **1a**. Because the optical rotation of natural **1a** was not documented by Seip and Hecker, the absolute configuration of natural **1a** is not unambiguously assignable. However, considering that the absolute configuration of C-4 and C-15 of all known jatrophanes is strictly conserved without exception and corresponds to the configuration of our synthetic **1a**,[1,53] it appears likely that natural **1a** and the material we have synthesized possess the same absolute configuration.

Encouraged by the successful synthesis of (−)-**1a**, we decided to embark on the synthesis of the 5,6-epoxy-jatrophane **1b**, whose isolation from *Euphorbia characias* and structural characterization was also reported by Seip and Hecker in 1984 (Scheme 9).[6] We expected that a slight modification and extension of the successful endgame of the synthesis of **1a** from 3-*epi*-characiol (**2**) should pave the way to **1b**. Accordingly, the Mitsunobu inversion of the absolute

(44) For a recent example, see: George, J. H.; Baldwin, J. E.; Adlington, R. M. *Org. Lett.* **2010**, *12*, 2394–2397.
(45) Oikawa, Y.; Yoshioka, T.; Yonemitsu, O. *Tetrahedron Lett.* **1982**, *23*, 885–888.
(46) Michrowska, A.; Bujok, R.; Harutyunyan, S.; Sashuk, V.; Dolgonos, G.; Grela, K. *J. Am. Chem. Soc.* **2004**, *126*, 9318–9325.
(47) Scholl, M.; Ding, S.; Lee, C. W.; Grubbs, R. H. *Org. Lett.* **1999**, *1*, 953–956.
(48) (a) Schwab, P.; France, M. B.; Ziller, J. W.; Grubbs, R. H. *Angew. Chem., Int. Ed. Engl.* **1995**, *34*, 2039–2041. (b) Schwab, P.; Grubbs, R. H.; Ziller, J. W. *J. Am. Chem. Soc.* **1996**, *118*, 100–110.
(49) (a) Garber, S. B.; Kingsbury, J. S.; Gray, B. L.; Hoveyda, A. H. *J. Am. Chem. Soc.* **2000**, *122*, 8168–8179. (b) Gessler, S.; Randl, S.; Blechert, S. *Tetrahedron Lett.* **2000**, *41*, 9973–9976.
(50) Mitsunobu, O.; Yamada, M. *Bull. Chem. Soc. Jpn.* **1967**, *40*, 2380–2382.
(51) Sheehan, J.; Cruickshank, P.; Boshart, G. *J. Org. Chem.* **1961**, *26*, 2525–2528.
(52) Procopiou, P. A.; Baugh, S. P. D.; Flack, S. S.; Inglis, G. G. A. *J. Org. Chem.* **1998**, *63*, 2342–2347.
(53) For the first determination of the absolute configuration of a jatrophane diterpene by X-ray crystallography, see: Yamamura, S.; Kosemura, S.; Ohba, S.; Ito, M.; Saito, Y. *Tetrahedron Lett.* **1981**, *22*, 5315–5318.

configuration of C3 was performed with benzoic acid, as the resulting benzoic acid ester is part of the natural product. The remaining tertiary hydroxyl group was then esterified under the approved conditions (Bz_2O or Ac_2O, catalytic TMSOTf) to deliver the non-natural characiol diester **31** and the corresponding acetate, which was subjected to a Prilezhaev epoxidation[54] to provide the natural product **1b** as a single diastereomer. The result of the epoxidation came as no surprise, because Seip and Hecker had shown that the diester **1a** of characiol could be epoxidized with *m*-CPBA to afford the corresponding 5,6-epoxide of **1a** diastereoselectively.[6] The available ^{1}H and ^{13}C NMR data of natural **1b** are fully consistent with the data we recorded for synthetic **1b**. The optical rotation of synthetic **1b** is −20.6° (*c* 0.34, $CHCl_3$); however, again no literature value is available for **1b** and our attempts to unambiguously assign the configuration of the epoxide moiety by NOE studies were inconclusive. The original structural assignment of the natural product **1b** by Seip and Hecker rests upon the comparison of the ^{1}H and ^{13}C NMR data with those of a structurally related diester (3-*O*-isobuturyl-15-*O*-acetyl) of the lathyrane diterpene 5,6-epoxy-jolkinol. However, their assignment of the (5*S*,6S)-configuration to the epoxide moiety in this natural product is in contradiction to the work of Uemura, who proposed the 5*R*,6*R* configuration for a related monoester (15-*O*-cinnamoyl) of jolkinol on the basis of chemical correlation.[55] Fortunately, the assignment of Uemura later became trustworthy because of two independent NOE studies.[56] Thus, considering all available information, we suggest that the structure for the natural product **1b** depicted in Scheme 9, including the absolute configuration 2*S*,3*S*,4*S*,5*R*,6*R*, is accurate.

We expanded the synthetic part of our study by exploiting the established route to 3-*epi*-characiol (**2**) for the synthesis of non-natural jatropha-5,12-dienes and focused our attention on creating structural diversity with respect to the nature of the acyloxy substituent at C3 (Scheme 10). Thus, esterification of **2** with a small number of commercially available acids under the previously established conditions delivered the esters **33**−**36** as well as the bis(benzoate) **32**.

Evaluation as MDR Modulators. Previous reports have demonstrated the ability of jatrophane diterpenes to inhibit the multidrug resistance (MDR) associated transport protein ABCB1 (P-glycoprotein, P-gp);[57,58] thus, our 18 synthetic jatrophanes were subjected to a corresponding biological study.[59] Additionally, the effect of the jatrophanes on ABCG2 (breast cancer resistance protein, BCRP) and ABCC1

SCHEME 10. Synthesis of Non-Natural Derivates

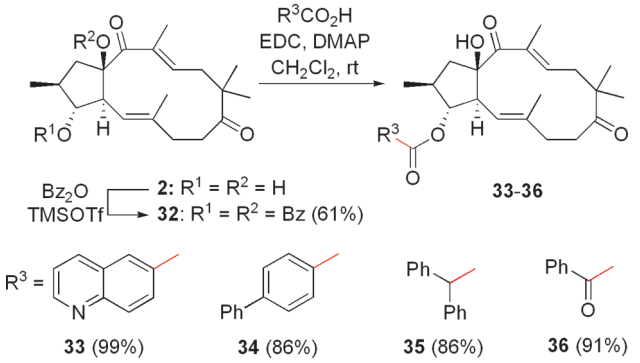

(multidrug resistance associated protein, MRP1), two other prominent ABC transporters involved in the development of multidrug resistance, was also investigated.

Initial studies with respect to ABCG2 and ABCC1 activity demonstrated that only **S9**[60] and **S10** were able to significantly inhibit the ABCC1-mediated efflux of calcein-AM out of 2008 MRP1 cells in concentrations up to 10 μmol/L and only **33**−**35** significantly affected ABCG2 transport activity.[61] Experimentally, we found that compounds **33**−**35**, having a larger aromatic substituent at C-3, possessed inhibitory activity, whereas the presence of the smaller benzoyl residue at C-3 (**S6**, **30**−**32**) is not sufficient to cause a significant reduction of ABCG2 activity.

As initially planned, we focused our experiments on the evaluation of jatrophane diterpenes as inhibitors of the transport protein ABCB1. Notably, the most potent synthetic jatrophane **33** possessed an inhibitory potency comparable to that of the first-generation inhibitor verapamil (Figure 4A).[62] In general, the presence of a lipophilic aromatic substituent at C-3 seems to enhance the ABCB1 inhibitory activity (e.g., **29** vs **30** or **S11** vs **S12**). Comparison of the compounds **29** (OH at C-3 and C-15), **30** (BzO at C30, OH at C-15), and **31** (BzO at C-3 and C-15) revealed an increasing inhibitory activity. The synthetic jatrophanes **1b**, **S8**, and **S10**, containing a 5,6-oxirane, are less active than the corresponding olefins (**S6**, **1a**, **S9**). Compounds containing a free hydroxyl group (**2**, **29**) or carbonyl group (**S7**) at C-3 are inactive.

As a direct correlation between overall lipophilicity and ABCB1 interaction has been postulated for different groups of structurally related substances, including jatrophane diterpenes, we calculated the octanol−water partition coefficients of the tested compounds. A significant correlation between log P_{calcd} and the ABCB1 inhibition caused by 10 μmol/L of the substances was observed (Figure 4B). It has been postulated in various studies that ABCB1 substrates or modulators enter the

(54) Prilezhaev, N. *Ber. Bunsen-Ges. Phys. Chem.* **1909**, *42*, 4811–4815.
(55) Uemura, D.; Nobuhara, K.; Nakayama, Y.; Shizuri, Y.; Hirata, Y. *Tetrahedron Lett.* **1976**, *17*, 4593–4596.
(56) (a) Itokawa, H.; Ichihara, Y.; Yahagi, M.; Watanabe, K.; Takeya, K. *Phytochemistry* **1990**, *29*, 2025–2026. (b) Duarte, N.; Varga, A.; Cherepnev, G.; Radics, R.; Molnár, J.; Ferreira, M. J. U. *Bioorg. Med. Chem.* **2007**, *15*, 546–554.
(57) (a) Hohmann, J.; Molnár, J.; Rédei, D.; Evanics, F.; Forgo, P.; Kálmán, A.; Argay, G.; Szabó, P. *J. Med. Chem.* **2002**, *45*, 2425–2431. (b) Corea, G.; Fattorusso, E.; Lanzotti, V.; Taglialatela-Scafati, O.; Appendino, G.; Ballero, M.; Simon, P.-N.; Dumontet, C.; Di Pietro, A. *J. Med. Chem.* **2003**, *46*, 3395–3402.
(58) For recent reviews on ABC transport proteins, see: (a) Colabufo, N. A.; Berardi, F.; Cantore, M.; Contino, M.; Inglese, C.; Niso, M.; Perrone, R. *J. Med. Chem.* **2009**, *53*, 1883–1897. (b) Eckford, P. D. W.; Sharom, F. J. *Chem. Rev.* **2009**, *109*, 2989–3011.
(59) ABCB1 transport activity was determined using the calcein-AM assay as described in the Supporting Information.
(60) See the Supporting Information for structural information on compounds labeled **S**.
(61) The fluorescent dye Hoechst 33342 was used for detecting ABCG2 inhibition. **33** effected about 70% inhibition of Hoechst 33342 efflux at a concentration of 10 μmol/L.
(62) A significant increase in the intracellular accumulation of calcein-AM was also detected in the presence of 10 μmol/L **34** and **35**, but an effect of a similar order of magnitude could also be observed in wild-type cells lacking ABCB1. Accordingly, their effect on ABCB1 cannot be finally estimated.
(63) (a) Rosenberg, M. F.; Velarde, G.; Ford, R. C.; Martin, C.; Berridge, G.; Kerr, I. D.; Callaghan, R.; Schmidlin, A.; Wooding, C.; Linton, K. J.; Higgins, C. F. *EMBO J.* **2001**, *20*, 5615–5625. (b) Aller, S. G.; Yu, J.; Ward, A.; Weng, Y.; Chittaboina, S.; Zhuo, R.; Harrell, P. M.; Trinh, Y. T.; Zhang, Q.; Urbatsch, I. L.; Chang, G. *Science* **2009**, *323*, 1718–1722.

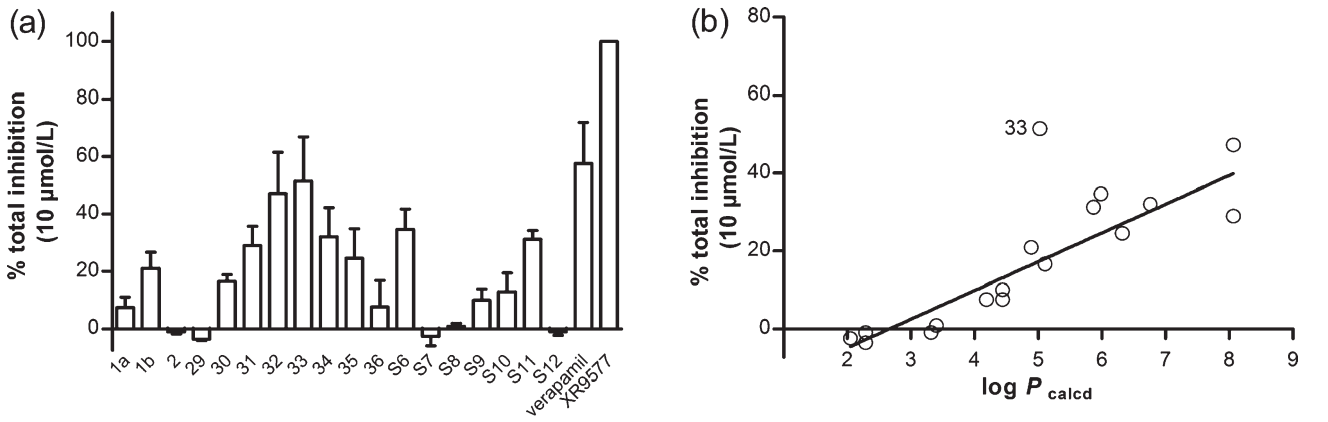

FIGURE 4. (a) ABCB1-inhibiting potency of all synthesized natural and non-natural jatrophanes determined by the calcein-AM (cal-AM) accumulation assay using ABCB1 overexpressing human A2780 Adr ovarian cancer cells. The increase in intracellular cal-AM accumulation was determined in the presence of 10 μmol/L of jatrophane diterpenes or the standard MDR reversing agents verapamil and XR9577 (total inhibition). The most potent substances are approximately as potent as verapamil. (b) Scatter plot of log *P* values and percentage of ABCB1 inhibition of the jatrophane diterpenes. A good correlation between lipophilicity and total inhibition can be observed ($r^2 = 0.704$). For **S6**−**S12** see the Supporting Information.

drug binding pocket directly from the plasma membrane.[63] As a consequence, lipophilic drugs accumulating in the membrane bilayer can easily bind and therefore possess an increased apparent affinity toward ABCB1. Interestingly, **33** exerted a relative total inhibition which could not be exclusively explained by its lipophilicity. The Brønsted basic nitrogen atom of the quinoline residue possibly supports specific binding of **33** to ABCB1, leading to an increased inhibition of the transporter. Further studies are required to verify this hypothesis.

An interesting dependence of the biological activity on the absolute configuration at C-3 was observed because the 3*R*-configured benzoic acid ester **32** was more active than its 3*S*-configured diastereomer **31**. Notably, the natural 3*S* configuration is highly conserved within the jatrophane diterpene family, making the 3*R* configuration accessible only by synthesis. The jatropha-5,12-dienes **31** and **32** represent the only truly diastereomeric pair of compounds investigated so far, and therefore, a reliable conclusion concerning the configuration−activity relationship cannot be drawn yet; clearly, further studies are indicated to explore the pharmacological opportunities hidden within the three-dimensional jatrophane scaffold.

Conclusions

We have reported the details of the successful total synthesis of the jatropha-5,12-diene diterpenes **1a**,**b** as well as of an ensemble of non-natural derivatives. The key step for the diastereoselective formation of the cyclopentane element was studied by DFT calculations. The results of the calculations provide a reasonable explanation for the observed substrate-induced diastereoselecitvity and support the usage of the B1B95 functional for future studies on the intramolecular carbonyl−ene reaction of α-keto esters. Subsequent biological studies demonstrated that the most potent compound (**33**) from this compound collection possess a MDR reversing potency comparable to that of the standard inhibitor verapamil.[64] In addition to **33**, a compound that also possessed inhibitory activity toward ABCB1 and ABCG2, several other jatrophanes containing lipophilic residues were selectively active with respect to ABCB1. Thus, non-natural 3-*epi*-characiol (**2**) would seem to represent a promising gateway for the development of selective inhibitors of ABCB1. Efforts toward the synthesis of additional natural and non-natural jatrophane diterpenes and their biological evaluation are currently ongoing in our laboratories.

Experimental Section

Ketone 22. TEMPO (1 mg, 0.006 mmol, 0.6 equiv) and PhI(OAc)$_2$ (19 mg, 0.059, 5.5 equiv) were added at room temperature to a solution of the diol **19b** (6 mg, 0.011 mmol, 1 equiv) in CH_2Cl_2 (0.6 mL, 55 mL/mmol of **19b**). After it was stirred for 1 h at ambient temperature, the reaction mixture was diluted with cyclohexane. After concentration under reduced pressure and chromatographic purification (cyclohexane/ethyl acetate 10/1) of the crude product, the ketone **22** (3 mg, 0.006 mmol, 52%) was obtained as a light yellow oil. **22** was isolated as a 1:1 mixture of C9 epimers: R_f 0.79 (cyclohexane/ethyl acetate 2/1); ^{1}H NMR (400 MHz, $CDCl_3$) δ −0.01 (s, 3 + 3H), 0.08 (s, 3 + 3H), 0.88 (s, 9 + 9H + 3 + 3H), 0.93 (s, 3 + 3H), 1.15 (d, ^3J = 6.3 Hz, 3 + 3H), 1.55−1.72 (m, 2 + 2H), 1.65 (s, 3 + 3H), 1.82 (dd, ^3J = 12.0 Hz, ^2J = 18.6 Hz, 1 + 1H), 2.01−2.19 (m, 4 + 4H), 2.30−2.37 (m, 1 + 1H), 2.59 (dd, ^3J = 8.1 Hz, ^2J = 18.6 Hz, 1 + 1H), 3.04−3.12 (m, 2 + 2H), 3.60 (dd, $^3J_1$ = 8.9 Hz, $^3J_2$ = 17.4 Hz, 1 + 1H), 3.80 (s, 3 + 3H), 4.51−4.56 (m, 2 + 2H), 4.93 (d, ^3J = 8.2 Hz, 1 + 1H), 4.99−5.04 (m, 2 + 2H), 5.79−5.90 (m, 1 + 1H), 6.87 (d, ^3J = 8.5 Hz, 2 + 2H), 7.28 (d, ^3J = 8.5 Hz, 2 + 2H); ^{13}C NMR (101 MHz, $CDCl_3$) δ −4.3 (1 + 1CH_3), −3.9 (1 + 1CH_3), 17.2 (1 + 1CH_3), 17.6 (1 + 1CH_3), 18.0 (1 + 1C), 23.6 (2 + 2CH_3), 25.9 (3 + 3CH_3), 29.5 (1 + 1CH_2), 37.7 (1 + 1C), 38.4 (1 + 1CH), 39.1 (1 + 1CH_2), 43.8 (1 + 1CH_2), 45.1 (1 + 1CH_2), 55.3 (1 + 1CH_3), 59.5 (1 + 1CH), 74.6 (1 + 1CH_2), 82.6 (1 + 1CH), 86.8 (1 + 1CH), 113.7 (2 + 2CH), 117.0 (1 + 1CH_2), 119.6 (1 + 1CH), 129.1 (2 + 2CH), 131.4 (1 + 1C), 135.6 (1 + 1CH), 141.8 (1 + 1C), 159.0 (1 + 1C), 215.0 (1 + 1C); IR (film on KBr) ν 2955, 2930, 2855, 1745, 1615, 1515, 1465, 1385, 1360, 1250, 1120, 1100, 1040, 865, 835, 775 cm^{-1}; HRMS (ESI) *m*/*z* calcd for $C_{32}H_{53}O_4Si$ ([M + H]$^+$) 529.3708, found 529.3704.

α-Hydroxy Ketone 23. H_2C=C(Me)MgBr (0.78 mL, 0.5 M in THF, 0.39 mmol, 2.5 equiv) was added to a cooled (0 °C) solution of the aldehyde **20** (87 mg, 0.156 mmol, 1 equiv) in THF (1 mL, 6.4 mL/mmol **20**). The solution was stirred for 30 min at 0 °C. Saturated aqueous NH_4Cl solution was added, followed

(64) Tsuruo, T.; Iida, H.; Tsukagoshi, S.; Sakurai, Y. *Cancer Res.* **1981**, *41*, 1967–1972.

by the separation of the phases and the extraction of the aqueous phase with CH_2Cl_2 (4×). The combined organic phases were dried ($MgSO_4$) and concentrated under reduced pressure. Purification by chromatography (cyclohexane/ethyl acetate 20/1) afforded the α-hydroxy ketone **23** (59 mg, 0.106 mmol, 68%) as a light yellow oil. **23** was obtained as a mixture of C9/C14 epimers: R_f 0.63 (cyclohexane/ethyl acetate 2/1); ^{1}H NMR (400 MHz, $CDCl_3$) δ 0.10 (s, 3H), 0.15 (s, 3H), 0.87 (s, 3H), 0.91 (s, 3H), 0.93 (s, 9H), 0.95 (d, ^3J = 8.0 Hz, 3H), 1.42 (s, 1H), 1.45−1.63 (m, 2H), 1.66 (s, 3H), 1.92−2.02 (m, 2H), 2.09−2.14 (m, 1H), 2.19−2.27 (m, 2H), 2.32−2.43 (m, 1H), 2.95−3.02 (m, 2H), 3.21−3.33 (m, 1H), 3.41−3.49 (m, 1H), 3.77−3.81 (m, 3H), 4.48−4.51 (m, 2H), 4.77−4.81 (m, 2H), 4.98−5.04 (m, 2H), 5.77−5.88 (m, 1H), 6.86−6.89 (m, 2H), 7.25−7.28 (m, 2H); ^{13}C NMR (101 MHz, $CDCl_3$) δ −4.8 (CH_3), −4.5 (CH_3), 16.5 (CH_3), 18.0 (C), 19.0 (CH_3), 23.6 (2 × CH_3), 25.8 (3 × CH_3), 29.4 (CH_2), 37.9 (CH_2), 39.1 (C), 40.3 (CH), 41.5 (CH_2), 43.8 (CH_2), 51.1 (CH), 55.4 (CH_3), 73.5 (CH), 74.5 (CH_2), 76.1 (CH), 86.6 (CH), 113.8 (2 × CH), 117.0 (CH_2), 119.7 (CH), 128.9 (2 × CH), 131.4 (C), 135.5 (CH), 139.5 (C), 159.1 (C), 212.1 (C); IR (film on KBr) ν 2955, 2930, 2855, 1715, 1515, 1470, 1465, 1250, 1075, 1040, 835, 775 cm^{-1}; HRMS (ESI) m/z calcd for $C_{33}H_{55}O_5Si$ ($[M + H]^+$) 559.3813, found 559.3810.

15-*O*-Acetyl-3-*O*-benzoylcharaciol (5*R*,6*R*)-Oxide (1b). *m*-CPBA (5 mg, 0.029 mmol, 2 equiv) was added at room temperature to a solution of 15-*O*-acetyl-3-*O*-benzoylcharaciol (**S6**;[61] 7 mg, 0.015 mmol, 1 equiv) in CH_2Cl_2 (2 mL, 48 mL/mmol of **S6**). The reaction mixture was stirred for 15 h at ambient temperature and then diluted with saturated aqueous $Na_2S_2O_3$ solution. The phases were separated, and the aqueous layer was extracted with CH_2Cl_2 (3×). The combined organic phases were dried ($MgSO_4$) and concentrated under reduced pressure. Purification of the residue by chromatography (cyclohexane/ethyl acetate 5/1 to 2/1) provided 15-*O*-acetyl-3-*O*-benzoylcharaciol (5*R*,6*R*)-oxide (**1b**; 5 mg, 0.01 mmol, 69%) as a white solid (mp 187 °C): R_f 0.33 (cyclohexane/ethyl acetate 2/1); ^{1}H NMR (peak assignments were deduced from ^{1}H−^{1}H COSY spectra and are listed on the basis of the jatrophane numbering; 400 MHz, $CDCl_3$) δ 0.97 (d, ^3J = 6.5 Hz, 16-CH_3), 1.04 (s, 18-CH_3), 1.08 (s, 19-CH_3), 1.28 (s, 17-CH_3), 1.72 (dd, ^3J = ^2J = 13.6 Hz, 1-CH_2, 1H^{Re}), 1.77 (s, 20-CH_3), 1.87 (dd, $^3J_1$ = 3.8 Hz, $^3J_2$ = 8.9 Hz, 4-CH), 1.92−2.04 (m, 8-CH_2), 2.15−2.29 (m, 2-CH + 7-CH_2, 1H^{Si}), 2.27 (s, acetate-CH_3), 2.42−2.55 (m, 11-CH_2), 2.84−2.91 (m, 7-CH_2, 1H^{Re}), 3.33 (dd, ^3J = 7.3 Hz, ^2J = 13.6 Hz, 1-CH_2, 1H^{Si}), 3.39 (d, ^3J = 8.9 Hz, 5-CH), 5.67 (dd, $^3J_1$ = $^3J_2$ = 3.8 Hz, 3-CH), 6.04−6.07 (m, 12-CH), 7.49 (dd, $^3J_1$ = $^3J_2$ = 7.5 Hz, 2 × CH_{ar}), 7.61 (dd, $^3J_1$ = $^3J_2$ = 7.5 Hz, CH_{ar}), 8.09 (d, $^3J_1$ = 7.5 Hz, 2 × CH_{ar}); ^{13}C NMR (101 MHz, $CDCl_3$) δ 12.2 (CH_3), 13.6 (CH_3), 16.8 (CH_3), 21.5 (CH_3), 23.3 (CH_3), 25.1 (CH_3), 32.1 (CH_2), 32.9 (CH_2), 38.6 (CH), 39.4 (CH_2), 47.9 (CH_2), 48.0 (C), 51.5 (CH), 59.4 (CH), 61.4 (C), 80.7 (CH), 90.1 (C), 128.5 (2 × CH), 129.8 (2 × CH), 130.3 (C), 133.1 (CH), 135.6 (CH), 136.9 (C), 165.5 (C), 170.3 (C), 199.9 (C), 213.6 (C); IR (film on KBr) ν 2970, 2930, 1720, 1670, 1385, 1270, 1245, 1110, 710 cm^{-1}; HRMS (ESI) m/z calcd for $C_{29}H_{37}O_7$ ($[M + H]^+$) 497.2534, found 497.2529; $[\alpha]^{25}_D$ = −20.6° (*c* 0.34, $CHCl_3$).

Acknowledgment. Financial support of this work was provided by the Deutsche Forschungsgemeinschaft (HI 628/6) and the Technische Universität Dortmund. Computer time was provided by the IT & Medien Centrum of the TU Dortmund. C.S. thanks Henrik Scholz and Benjamin Wanitschka (both of the TU Dortmund) for skillful technical assistance.

Supporting Information Available: Text, tables, and figures giving computational details, experimental chemical and biological procedures, spectral and analytical data, and ^{1}H and ^{13}C NMR spectra for all new compounds. This material is available free of charge via the Internet at http://pubs.acs.org.